CHIN. PHYS. LETT. Vol. 27, No. 4 (2010) 044209

Spatial Splitting and Intensity Suppression of Four-Wave Mixing in V-Type Three-Level Atomic System *

LI Chuang-She(李创社), YIN Wei-Tao(尹伟涛), YUAN Chen-Zhi(袁晨智), SHI Mei-Zhen(史美震), ZHAO Yan(赵燕), ZHANG Yan-Peng(张彦鹏)**

Key Laboratory for Physical Electronics and Devices of the Ministry of Education, and Shaanxi Key Lab of Information Photonic Technique, Xi'an Jiaotong University, Xi'an 710049

(Received 8 December 2009)

We illustrate our experimental observation of coexisting the controllable spatial splitting and intensity suppression of four-wave mixing (FWM) beam in a V-type three-level atomic system. The peak number and separation distance of the FWM beam are controlled by the intensities and frequencies of the laser beams, as well as atomic density.

PACS: 42. 50. Gy, 42. 65. Jx, 42. 65. Tg DOI: 10.1088/0256-307X/27/4/044209

In the past few years, interesting effects such as induced focusing of optical beams,[1] beam shift and splitting,[2] and enhanced Kerr effect[3] have been experimentally demonstrated in two-level atomic systems. The atomic coherence can significantly enhance and modify the self- and cross-Kerr nonlinearities as well as four-wave mixing (FWM) processes in several multilevel atomic systems.[4−10] Such cross-Kerr nonlinear effects lead to the spatial modulation of the probe beam.[1,2] Recently, we experimentally observed the strong spatial shift and splitting of probe and generated FWM beams in a two-level system.[11−13] The coexisting spatial splitting and intensity suppression of the FWM beam in a V-type three-level system will be discussed in this work.

In this Letter, by arranging laser beams as illustrated in Fig. 1(a), we demonstrate the spatial splitting of the FWM signal owing to the cross-Kerr effect induced by the control field. Furthermore, the coexisting spatial splitting and intensity suppression of FWM induced by the proper dressing field and control field are also achieved. We also compare the spatial splitting phenomenon in different atomic systems.

Three energy levels ($|0\rangle$ $(3S_{1/2})$, $|1\rangle$ $(3P_{1/2})$ and $|2\rangle$ $(3P_{3/2})$) in Na atoms form V-type three-level atomic system as shown in Fig. 1(b). The laser beams $\boldsymbol{E}_2$ and $\boldsymbol{E}_2'$ (with Rabi frequencies G_2 and G_2' respectively) can be scanned to connect either the transition from $|0\rangle$ to $|1\rangle$ in the V-type three-level or the transition from $|0\rangle$ to $|2\rangle$ in the two-level atomic systems. While the dressing beam $\boldsymbol{E}_1'$ and the probe beam $\boldsymbol{E}_3$ (with G_1' and G_3 respectively) connect the transition from $|0\rangle$ to $|2\rangle$ in both the atomic systems. The generated FWM beam $\boldsymbol{E}_{\rm F2}$ (with Rabi frequency $G_{\rm F2}$) connect the transition from $|0\rangle$ to $|2\rangle$.

The experiment was carried out with Na vapor in a 18-cm-long heat pipe. The four laser beams come from two dye lasers (10 Hz rate, 5 ns pulse width, and 0.04 $\rm cm^{-1}$ linewidth), the control beam $\boldsymbol{E}_2'$ and beam $\boldsymbol{E}_2$ with the frequency ω_2, the dressing beam $\boldsymbol{E}_1'$ and beam $\boldsymbol{E}_3$ with ω_1. As shown in Fig. 1(a), the pulse laser beams (horizontally polarized) with diameters of about 1 mm are aligned spatially with the control beams $\boldsymbol{E}_2(\boldsymbol{k}_2)$ and $\boldsymbol{E}_2'(\boldsymbol{k}_2')$ propagating through the atomic medium in the same direction with small angles (0.3°). The probe beam $\boldsymbol{E}_3$ $(\boldsymbol{k}_3)$ propagates in the opposite direction of $\boldsymbol{E}_2$. Satisfying the phase-matching condition $\boldsymbol{k}_{\rm F2} = \boldsymbol{k}_2 - \boldsymbol{k}_2' + \boldsymbol{k}_3$, a generated FWM beam $\boldsymbol{E}_{\rm F2}$ which propagates along the opposite direction of beam $\boldsymbol{E}_2'$ is monitored by a charge coupled device (CCD).

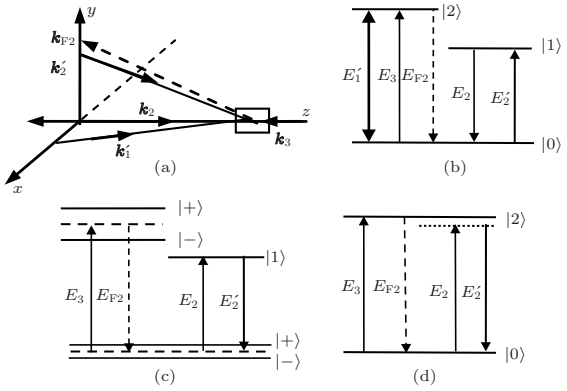


Fig. 1. (a) Spatial beam geometry used in the experiments with four laser beams. (b) Energy-level diagram of a V-type three-level and (c) the corresponding dressed-state picture, (d) energy-level diagram of a two-level atomic system.

*Supported by the National Natural Science Foundation of China under Grant No 10974151, the New Century Excellent Talent Project (NCET) of the Ministry of Education of China under Grant No 08-0431, the Cross-Disciplinary Project of Xi'an Jiaotong University under Grant No 2009xjtujc08.

**Email: ypzhang@mail.xjtu.edu.cn

© 2010 Chinese Physical Society and IOP Publishing Ltd

As shown in Fig. 1(a), beams $\boldsymbol{E}_2$, $\boldsymbol{E}_2'$, $\boldsymbol{E}_3$ and $\boldsymbol{E}_{\rm F2}$ are all in the yoz plane. The dressing field $\boldsymbol{E}_1'$ propagates in the xoz plane, and the intensity is approximately 5 times larger than the control beam $\boldsymbol{E}_2'$, 50 times larger than $\boldsymbol{E}_2$, 100 times larger than $\boldsymbol{E}_{\rm F2}$ and the probe beam $\boldsymbol{E}_3$. Thus, the dressing beam $\boldsymbol{E}_1'$ can split the resonance levels $|0\rangle$ and $|2\rangle$ into dressed-state $|\pm\rangle$, respectively. Since it does not overlap with the FWM beam $\boldsymbol{E}_{\rm F2}$, it only leads to the suppression of the FWM signal intensity. While $\boldsymbol{E}_2'$ almost overlaps with $\boldsymbol{E}_{\rm F2}$ and the induced cross-Kerr nonlinear effect causes the splitting of the $\boldsymbol{E}_{\rm F2}$ beam spot.

The $\boldsymbol{E}_{\rm F2}$ process is dressed by $\boldsymbol{E}_1'$ in a V-type three-level system, we can easily obtain $\rho_{\rm F2} = -iG_3G_2'^2/[d_1d_2(d_1+G_2'^2/d_2)]$ for FWM signal intensity by solving the coupled density-matrix equations under the weak field approximation, here $d_1 = i\Delta_1 + \Gamma_{10}$, $d_2 = \Gamma_1 + i(\Delta_1 - \Delta_2)$. On the other hand, for cross-Kerr coefficients of the FWM beam $\boldsymbol{E}_{\rm F2}$, we have $\rho_{10}^{(3)} = \rho_a = -iG_a/[d_1\Gamma_1(d_1 + G_1'^2/\Gamma_0 + G_1'^2/\Gamma_1)]$, $\rho_{10}^{(3)} = \rho_b = -iG_b/[d_1d_2(d_1+G_2'^2/d_2)]$ and $\rho_{10}^{(3)} = \rho_c = -iG_c/(d_1d_2d_3)$, respectively, where $G_a = G_{\rm F2}G_1'^2$, $G_b = G_{\rm F2}G_2'^2$, $G_c = G_{\rm F2}G_{1,2}'^2$.

The beam splitting can be described by the nonlinear Schrodinger equation

$$\frac{\partial A_{\rm F2}}{\partial z} - \frac{i\nabla_\perp^2 A_{\rm F2}}{2k_{\rm F2}} = \frac{ik_{\rm F2}}{n_0}\Big[n_2^S|A_{\rm F2}|^2 + 2n_2^{X1}|A_2'|^2 + 2n_2^{X2}|A_1'|^2\Big]A_{\rm F2}, \quad (1)$$

where z is the longitudinal coordinate, $k_{\rm F2} = \omega_1 n_0/c$, n_0 is the linear refractive index, n_2^S are the self-Kerr coefficient of $\boldsymbol{E}_{\rm F2}$, $n_2^{X1,X2}$ are the cross-Kerr coefficients of $\boldsymbol{E}_{\rm F2}$ induced by $\boldsymbol{E}_2'$ and $\boldsymbol{E}_1'$, respectively. $A_{\rm F2}$, A_1', and A_2' are the slowly varying envelope amplitudes of beams $\boldsymbol{E}_{\rm F2}$, $\boldsymbol{E}_1'$, and $\boldsymbol{E}_2'$, respectively. Assuming that input lasers are Gaussian profiles, Eq. (1) can be numerically solved with the split-step method. For a self-defocusing medium the Kerr coefficient is negative, while for a self-focusing one it is positive. We can obtain the nonlinear phase shift $\phi_{\rm NL}(z,x) = \frac{2k_{\rm F2}n_2}{n_{0({\rm F2})}} Ie^{-(w_0'x)^2}z$, where $n_2 = C{\rm Re}\chi^{(3)}$, $C = (\varepsilon_0 cn_0)^{-1}$, the susceptibility $\chi^{(3)} = D\rho_{10}^{(3)}$ and $D = N\mu_{10}^4/(\hbar^3\varepsilon_0 G_{\rm F2}G_i^2)$. N is the atomic density in the sample cell and μ_{10} is the dipole matrix element between $|0\rangle$ and $|2\rangle$.

The nonlinear phase shift $\phi_{\rm NL}(z,x)$ becomes larger with increasing n_2, and due to $|\boldsymbol{E}_{\rm F2}|^2 \propto \sin^2\phi_{\rm NL}$ more spatial splitting appears in the $\boldsymbol{E}_{\rm F2}$ beam profile. Figure 2 shows the spatial splitting evolution of $\boldsymbol{E}_{\rm F2}$ beam versus the frequency detuning Δ_1. Since $\boldsymbol{E}_2'$ is just below the $\boldsymbol{E}_{\rm F2}$ beam, the FWM signal beam is vertically split by $\boldsymbol{E}_2'$, as shown in Fig. 1(a). Correspondingly, the peak separation number in the $\boldsymbol{E}_{\rm F2}$ beam profiles increases from one to three while the nonlinear refractive index $|n_2|$ changes from the minimum to the maximum. There is no peak separation at the resonate frequency where n_2 approximates to zero. Apparently, when $|n_2|$ reaches the largest, we can obtain strong peak separation.

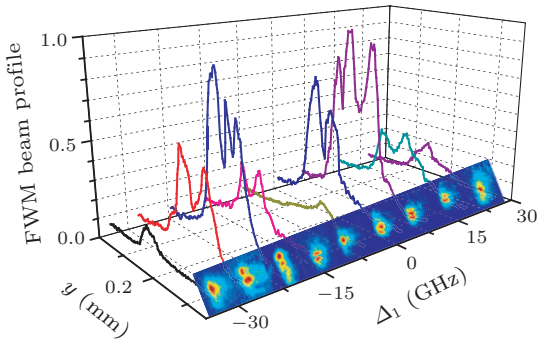


Fig. 2. $\boldsymbol{E}_{\rm F2}$ beam profiles versus Δ_1 at 250°C in a V-type three-level system. The parameters are $\Delta_2 = 0$, $G_1' = 0$ ($\boldsymbol{E}_1'$ is blocked), $G_3 = 0.1$ GHz, $G_2 = 1.9$ GHz, $G_2' = 20.8$ GHz.

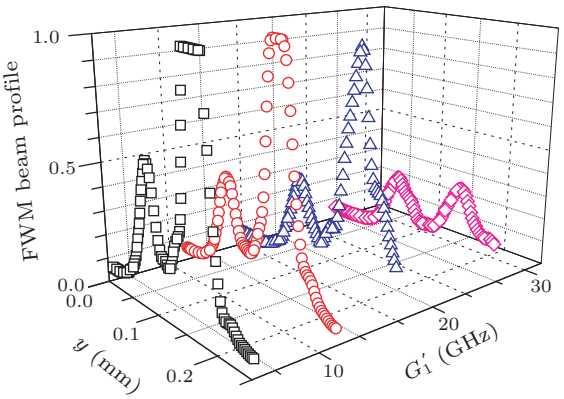


Fig. 3. $\boldsymbol{E}_{\rm F2}$ beam profiles with $G_1' = 6.8$ GHz (square), 13.8 GHz (circle), 19.7 GHz (triangle) and 20.6 GHz (diamond) at 265°C in a V-type three-level system. The other parameters are $\Delta_1 = 17$ GHz, $\Delta_2 = 0$, $G_3 = 0.1$ GHz, $G_2 = 1.5$ GHz, $G_2' = 10$ GHz.

Figure 3 shows the spatial splitting of the $\boldsymbol{E}_{\rm F2}$ beam profile when $\boldsymbol{E}_1'$ increases gradually. In fact, according to $\rho_{\rm F2} = -iG_3G_2'^2/(d_1d_2d_3)$, we can see that $\boldsymbol{E}_{\rm F2}$ is suppressed when $\boldsymbol{E}_1'$ becomes stronger. The reason is that $\boldsymbol{E}_1'$ breaks the resonance levels $|0\rangle$ and $|2\rangle$ into dressed-state $|\pm\rangle$ respectively, as shown in Fig. 1(c). Moreover, when $\boldsymbol{E}_1'$ is small and $\boldsymbol{E}_{\rm F2}$ is partly overlap with the laser beam $\boldsymbol{E}_2'$, the $\boldsymbol{E}_{\rm F2}$ beam splits into two asymmetric parts (the square, circle, and triangle curves). When $\boldsymbol{E}_1'$ is strong enough, the $\boldsymbol{E}_{\rm F2}$ beam have down shift induced by $\boldsymbol{E}_1'$ and overlap $\boldsymbol{E}_2'$. Thus the splitting of the FWM beam will be more balance, and two splitting parts turn almost the same at $G_1' = 20.6$ GHz (diamond curve).

As is known, the temperature influences the atomic density in the vapor medium which is proportional to the propagation distance z in $\phi_{\rm NL}(z,x) = \frac{2k_{\rm F2}n_2}{n_{0({\rm F2})}} Ie^{-(w_0'x)^2}z$. With increasing temperature, $\phi_{\rm NL}$

becomes larger, which indicates more spatial splitting in the FWM beam profile. To examine the temperature effect imposed on the FWM signal, the temperature in the vapor sample is increased gradually. Figure 4 shows intensity curves of FWM signals under different temperatures. The peak separation number of the FWM beam profiles increases as temperature rises. There are four separation peaks of the beam profile at 280°C.

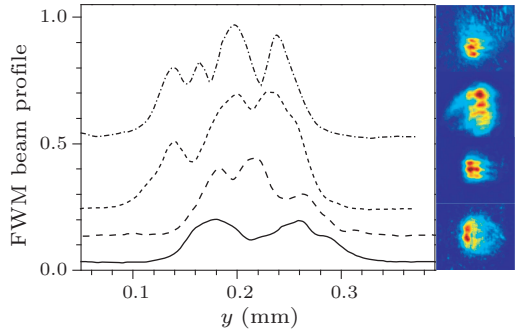


Fig. 4. $\boldsymbol{E}_{\rm F2}$ beam profiles in a V-type three level system at 230°C (solid curve), 240°C (dashed curve), 260°C (doted curve) and 280°C (dash doted curve). Inset: spots of $\boldsymbol{E}_{\rm F2}$ beam profile at 280°C to 230°C from top to bottom. The other parameters are $\Delta_1 = -10\,\text{GHz}$, $\Delta_2 = 0$, $G_3 = 0.1\,\text{GHz}$, $G_2 = 1.5\,\text{GHz}$, $G_2' = 10\,\text{GHz}$.

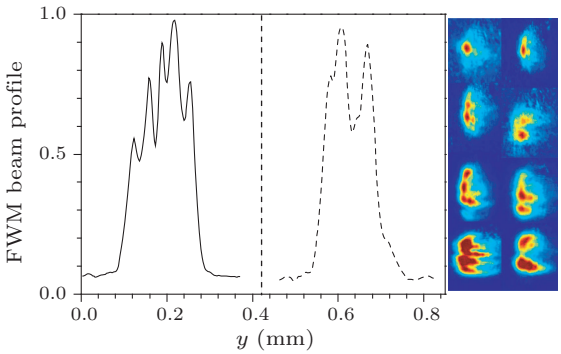


Fig. 5. $\boldsymbol{E}_{\rm F2}$ beam profiles in a two-level (solid) and V-type three-level (dash) atomic systems at 260°C. Curves: Intensities of $\boldsymbol{E}_{\rm F2}$ beams versus frequency detuning in a two-level (left) and V-type three-level (right) atomic systems at 230, 240, 260, and 280°C from top to bottom. The other parameters are $\Delta_1 = -10\,\text{GHz}$, $\Delta_2 = 0$, $G_3 = 0.1\,\text{GHz}$, $G_2 = 1.5\,\text{GHz}$, $G_2' = 10\,\text{GHz}$.

The different Kerr nonlinear index of refraction n_2 leads to the change of $\phi_{\rm NL}$ in the spatial phase expression which is represented by spatial splitting of the FWM beam. Since the dipole moment μ_{20} of transition $|0\rangle - |2\rangle$ is larger than the dipole moment μ_{10} transition $|0\rangle - |1\rangle$, we can deduce that the cross-Kerr coefficient n_2 in a two-level system is larger than that in a V-type three-level system.[11–13] We can see that the peak separation number of beam profile in a two-level system (solid curve) is more than that in a V-type three level system (dashed curve) for larger n_2. The inset in Fig. 5 shows the spatial splitting of $\boldsymbol{E}_{\rm F2}$ via n_2 in two different atomic energy-level systems at 230, 240, 260, and 280°C from top to bottom where all the spot-splitting in the two-level system is apparently larger than that in the V-type three-level system.

In conclusion, coexisting the spatial splitting and intensity suppression of FWM beam is observed in a V-type three-level system. The peak separation of the FWM beam are controlled by the intensities and frequencies of the laser beams, as well as atomic density. Such studies can have potential applications in soliton deflection and splitting communication, spatial optical switch and other quantum information processes.

References

[1] Agrawal G P 1990 *Phys. Rev. Lett.* **64** 2487
[2] Hickmann J M, Gomes A S L and de Araujo C B 1992 *Phys. Rev. Lett.* **68** 3547
[3] Li Y Q, Jin S Z and Xiao M 1995 *Phys. Rev.* A **51** 1754
[4] Wang H, Goorskey D and Xiao M 2001 *Phys. Rev. Lett.* **87** 073601
[5] Zhang Y P, Brown A W, and Xiao M 2007 *Phys. Rev. Lett.* **99** 123603
[6] Zhang Y P, Khadka U, Anderson B, and Xiao M 2009 *Phys. Rev. Lett.* **102** 013601
[7] Wu Y and Deng L 2004 *Phys Rev. Lett.* **93** 143904
[8] Wu Y, Yang X 2004 *Phys. Rev.* A **70** 053818
Wu Y 2005 *Phys. Rev. Lett.* **71** 053820
[9] Li C B, Nie Z Q, Zhang W F, Zhang Y P, Song J P, Li Y Y and Lu K Q 2008 *Chin. Phys. Lett.* **25** 4266
[10] Li P Z, Nie Z Q, Zhang Y P, Jiang T, Du Y G, Gan C L, Song J P and Lu K Q 2007 *Chin. Phys. Lett.* **24** 3420
[11] Zhang Y P, Zuo C C, Zheng H B, Li C B, Nie Z Q, Song J P, Chang H, Xiao M 2009 *Phys. Rev.* A **80** 055804
[12] Qi Y R, Gao H and Zhang S G 2009 *Chin. Phys. Lett.* **26** 114211
[13] Lu X S, Chen Q F, Shi B S and Guo G C 2009 *Chin. Phys. Lett.* **26** 064204